Yeuk Yin Lam
Math 4540
Professor Weiler
May 26th, 2022

Plateau's Problem: Minimal Surfaces

Introduction: A Brief History of Plateau's Problem

The Plateau's problem is that of finding a surface of minimal area with a fixed curve as its boundary (minimal surface). In 1760, the Swiss mathematician Leonhard Euler and the French mathematician Joseph Lagrange first posed the problem.[1] Physically, imagine a soap film bounded by a curve C. As a soap film has energy in the form of surface tension and the energy is proportional to the surface area, a soap film bounded by C should adopt the shape of a surface with least surface area (hence least surface tension and least energy to maintain the shape) with boundary C. For instance, a soap bubble is spherical because a sphere has the smallest surface area, subject to enclosing a given volume of air. Thus, Euler and Lagrange actually aimed to find energy-minimizing surfaces. In 1849, the Belgian physicist Joseph Plateau demonstrated that a minimal surface could be obtained by immersing a wire frame (representing the boundary) into soapy water. Later, in the early 20th century, the Hungarian-American mathematician Jesse Douglas proved the existence of a minimal solution for any given simple boundary, generalized Plateau's Problem, and demonstrated its general solutions by using calculus of variation. In 1976, the American mathematician Jean Taylor proved Plateau's conjecture that soap film surfaces can only intersect in two ways: three surfaces can intersect along a curve, meeting at equal angles of 120 degrees, or four surfaces can intersect at a point, meeting at about 109 degrees.[2] In other fields, for example in architecture, the German architect Frei Otto utilized the concept of minimal surfaces in his design of the West German pavilion in 1967. The following section offers a basic framework for studying Plateau's Problem and a corresponding example and theorem.

Basic Formulation, The Catenoid Example, and a Theorem

We study a family of surface patches $\sigma: U \to \mathbb{R}^3$, where U is an open subset of $\mathbb{R}^2$ independent of $\tau \in (-\delta, \delta)$ for some $\delta > 0$.[3] Let $\sigma = \sigma^0$ and the map $(u, v, \tau) \mapsto \sigma^\tau(u, v)$ be smooth. We define the surface variation of the family $\varphi: U \to \mathbb{R}^3$ to be given by $\varphi = \dot{\sigma^\tau}$ at $\tau = 0$. Further, let π be a simple closed curve contained in U alongside its interior $int(\pi)$, which means π corresponds to a closed curve $\gamma^\tau = \sigma^\tau \circ \pi$ in the surface patch σ^τ. Then, the area function $A(\tau)$ given by $A(\tau) = \int_{int(\pi)} dA_{\sigma^\tau}$ represents the area of the part of σ^τ inside γ^τ.

Now, we define a minimal surface be a surface whose mean curvature is zero everywhere. As a Corollary, if a surface S has least area among all surfaces with the same boundary curve, then S is a minimal surface. To illustrate our Corollary, we provide a numerical example of minimal surfaces. Consider the catenoid parametrized by the surface patch $\sigma(u, v) = (\cosh u \cos v, \cosh u \sin v, u)$. We calculate coefficients of the first and second fundamental forms to be $E = G = \cosh^2 u$, $F = 0$, $L = -1$, $M = 0$, $N = 1$. Using Corollary 8.1.3, we obtain that $H = \frac{LG - 2MF + NE}{2(EG - F^2)} = \frac{-\cosh^2 u + \cosh^2 u}{2\cosh^4 u} = 0$. Since the mean curvature of the catenoid $H = 0$ everywhere, we have that the catenoid is a minimal surface by definition.

However, the converse of our Corollary is false. Going back to the catenoid example, let us fix $a > 0$. Consider two surfaces of the catenoid: S, consisting of the part of the catenoid with $|z| < a$ bounded by two circles of radius $\cosh u$ in the planes $z = \pm a$, and S_0, consisting of two discs $x^2 + y^2 \leq \cosh^2 a$ in the planes $z = \pm a$ (see Figure 1a).

[1] William L Hosch, "Plateau Problem," Encyclopædia Britannica (Encyclopædia Britannica, inc.), accessed May 26, 2022, https://www.britannica.com/science/Plateau-problem.
[2] Alex Meadows, "Minimal Surfaces and Isoperimetric Problems in Mathematics," Soap film geometry, 2006, http://faculty.smcm.edu/ammeadows/create/.
[3] Andrew Pressley, *Elementary Differential Geometry*, 2nd ed. (Springer, 2012).

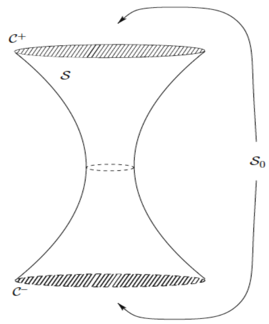

Figure 1a. A Catenoid, with Surfaces S and S_0

According to Proposition 6.4.2, the area of S is given by $\int_0^{2\pi}\int_{-a}^{a}(EG-F^2)^{1/2}\,dudv = \int_0^{2\pi}\int_{-a}^{a}\cosh^2 u\ dudv = 2\pi(a+\cosh a\sinh a)$. On the other hand, the area of S_0 is $2\pi\cosh^2 a$. Thus, the minimal surface S will not minimize the area among all surfaces with two circles of radius $\cosh u$ as boundary if $\cosh^2 a < a + \cosh a \sinh a$.

Now, we give the following theorem: assuming that the surface variation φ^τ vanishes along the boundary curve π, we have $\dot{A}(0) = -2\int_{int(\pi)} H(EG-F^2)^{1/2}\alpha\,dudv$, where H is the mean curvature of σ, E, F, G the coefficients of its first fundamental form, and $\alpha = \varphi \cdot N$, where N is the standard unit normal of σ. To give a simple proof, let $\varphi^\tau = \dot{\sigma^\tau}$ so that $\varphi^0 = \varphi$. There are smooth functions α^τ, β^τ, and γ^τ of (u,v,τ) such that $\varphi^\tau = \alpha^\tau N^\tau + \beta^\tau {\sigma_u}^\tau + \gamma^\tau {\sigma_v}^\tau$, so that $\alpha = \alpha^0$. Then, we have

$$A(\tau) = \int_{int(\pi)} \|\sigma_u \times \sigma_v\| dudv$$
$$\dot{A} = \int_{int(\pi)} \frac{\partial}{\partial\tau}\big(N\cdot(\sigma_u \times \sigma_v)\big)\,dudv \text{ (*)}.$$

We also have that

$$\frac{\partial}{\partial\tau}\big(N\cdot(\sigma_u \times \sigma_v)\big) = \dot{N}\cdot(\sigma_u \times \sigma_v) + N\cdot(\dot{\sigma_u} \times \sigma_v) + N\cdot(\sigma_u \times \dot{\sigma_v}).$$

We calculate that $\dot{N}\cdot(\sigma_u \times \sigma_v) = \dot{N}\cdot N\,\|\sigma_u \times \sigma_v\| = 0$. Further, using Proposition 6.4.2, we obtain $N\cdot(\dot{\sigma_u} \times \sigma_v) = \frac{G(\sigma_u\cdot\dot{\sigma_u}) - F(\sigma_v\cdot\dot{\sigma_u})}{(EG-F^2)^{1/2}}$ and $N\cdot(\sigma_u \times \dot{\sigma_v}) = \frac{E(\sigma_v\cdot\dot{\sigma_v}) - F(\sigma_u\cdot\dot{\sigma_v})}{(EG-F^2)^{1/2}}$. Moreover, using the facts that $\sigma_u\cdot N_u = -\sigma_{uu}\cdot N = -L$, $\sigma_u\cdot\sigma_{uu} = \frac{1}{2}E_u$ and $\sigma_u\cdot\sigma_{uv} = \frac{1}{2}E_v$, and $H = \frac{LG-2MF+NE}{2(EG-F^2)}$ (Corollary 8.1.3), and further simplifying, we finally obtain

$$\frac{\partial}{\partial\tau}\big(N\cdot(\sigma_u \times \sigma_v)\big) = (\beta(EG-F^2)^{1/2})_u + (\gamma(EG-F^2)^{1/2})_v - 2\alpha H(EG-F^2)^{1/2}.$$

If we compare this equation with (*), we see that we want to prove $\int_{int(\pi)}(\beta^0(EG-F^2)^{1/2})_u + (\gamma^0(EG-F^2)^{1/2})_v\,dudv = 0$. Using Green's Theorem, the integral above is equal to $\int_\pi (EG-F^2)^{1/2}(\beta^0 dv - \gamma^0 du)$, and this is equal to 0 since $\beta^0 = \gamma^0 = 0$. Thus, we have proven the theorem. The theorem tells us that if σ has the smallest area among all surfaces with the given boundary curve γ, then $\dot{A}(0) = 0$ for all smooth families of σ, which is satisfied only when the mean curvature $H = 0$, and hence the definition of the minimal surface with mean curvature zero everywhere.

Modern Development: Minmax Theory

When we search for minimal surfaces within a certain boundary, let us consider the space of all possible finite surfaces that live within the boundary.[4] Each point in this "surface space" maps to an entire surface in the original space (for example $\mathbb{R}^3$). If we think of each surface's area as the altitude of its corresponding point in the surface space, then finding minimal surfaces corresponds to finding saddle points in the topography of the surface space. For example, the equator, a closed geodesic, on a sphere represents a saddle point on the surface space because the half sphere it encloses is a minimal surface, while a smaller circle (than a great circle) on the sphere does not correspond to a saddle point on the surface space.

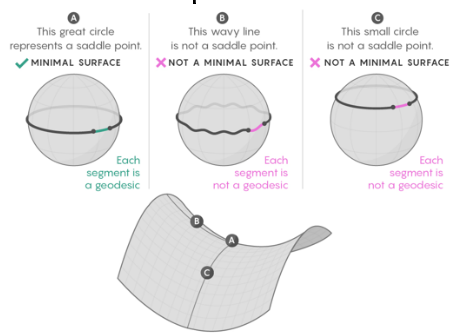

Figure 1b. The Surface Space (represented by the saddle)

The above describes the very rough idea of the Minmax Theory, proposed by Jon T. Pitts's dissertation in 1981. In an attempt to prove Willmore's conjecture that suggested that the roundest doughnut is the Clifford torus, mathematicians Fernando Codá Marques and André Neves utilized the Minmax Theory and were convinced that the Minmax Theory could be applied to much wider fields other than the Willmore conjecture. When Pitts first proposed the Minmax Theory, he conjectured that there could be an infinite list of saddle points, which would correspond to an infinite list of minimal surfaces within the original boundary. For example, there are infinitely many geodesics/great circles on a sphere, which means there are infinitely many saddle points in the surface space. In 2016, Marques and Neves showed that the infinite list of minmax surfaces, just as Pitts thought, behaved similar to the frequencies of a drum. In particular, they demonstrated that the areas of surfaces are roughly determined by the volume of the space they live in, instead of their boundary or shape. Further, in 2017, the two mathematicians proved that for most shapes, the minmax list contains infinitely many different minimal surfaces and constitute a dense space. Intuitively, in order for the space's volume to determine the areas of minimal surfaces, these surfaces somehow have to observe the entire volume. A couple of months later, they showed that as one goes out along the list of minmax surfaces, these surfaces tend to fill space evenly, a property named equidistribution. Other mathematicians have joined in the effort on further discoveries of the Minmax Theory. For example, Professor Xin Zhou built on Marques and Neves's work to prove that every minimal surface on Pitts's minmax list is different. Antoine Song, in 2018, also managed to show that every single shape in dimensions three through seven has infinitely many closed minimal surfaces. Recent progress in the Minmax Theory has been emerging one after another rapidly, and the Minmax Theory has evolved into a major direction in modern geometry and topology.

[4] Erica Klarreich, "Math Duo Maps the Infinite Terrain of Minimal Surfaces," Quanta, March 12, 2019, https://www.quantamagazine.org/math-duo-maps-the-infinite-terrain-of-minimal-surfaces-20190312/.

Blog: Minimal Surfaces in Architecture

Introduction

Throughout history, many architects have tried to infuse ideas of and embed structures of minimal surfaces into their projects. The famous German architect, Frei Otto, worked at the interface with engineering and found inspiration in self-organization and naturally evolving systems in nature.[5] With the belief that his architecture should have beautiful spaces, atmospheres, and be infused with elements of nature, Otto designed the Munich 1972 Olympic Roof, a floating cloud hovering above the landscape, based on the concept of minimal surfaces. Having done experiments with soap films, Otto again employed minimal surfaces in his design of the West German Pavilion. With regard to how the development of minimal surfaces and other geometric ideas play a role in architecture, Tobias Wallisser, an architect at the Laboratory for Visionary Architecture, explained, "a strong conceptual framework for the design is needed to develop coherent architectural designs. A great potential lies in the combination of intuitive ideas and vague formal explorations in combination with mathematically defined relationships and rule-based interdependencies." Indeed, architecture benefits a lot from minimal surfaces in a variety of ways, and different minimal surfaces bring different properties that become useful under distinct settings and construction needs. In this blog, we take a look at two specific minimal surfaces and their appearance in architecture: the Costa Minimal Surface and the helicoid.

Why Use Minimal Surfaces in Architecture?

Before going into specific examples of minimal surfaces in architecture, let us first get a sense of the geometric meaning of mean curvature and how it plays a role in minimal surfaces in architecture. Intuitively, the mean curvature measures how the volume of the submanifold locally changes under the flowing surface in the direction of the unit normal. Since by definition, a minimal surface has mean curvature $H = 0$ everywhere, the volume of the submanifold stays locally constant everywhere under the flowing surface in the direction of the unit normal. If we imagine a surface to be made up of many rubber bands, stretched out in all directions, then on a minimal surface, the forces due to the rubber bands balance out (the sum of all principal curvatures, which equals to the mean curvature, is zero everywhere), and the surface does not need to move to reduce surface tension.[6] This means that a minimal surface is able to minimize surface tension and creates equilibria of homogenous tension. Along with the fact that minimal surfaces are area minimizing, minimal surfaces are very material saving in the process of construction and energy conserving as well. They allow the building frame to become more lightweight, which can bring less safety hazards and require less structural support such as pillars and columns.[7] Therefore, minimal surfaces bring a lot of advantages to architecture, during both design and construction processes.

The Costa Minimal Surface and the Polvi Observatory

Until 1982, the world only knows three complete, embedded minimal surfaces of finite topology (meaning they have no boundaries and do not intersect themselves), all of which with genus 0 and diffeomorphic to a sphere: the plane, the catenoid, and the helicoid. In 1982, the Brazilian mathematician Celso Costa suggested the Costa Surface, a minimal embedding of genus 1 and three punctured square torus (see Figure 2 below). Its planar symmetry lines cut the surface into eight congruent squares and the straight lines through the saddle make up the diagonals of the squares.[8] Each of the pieces has a planar end and a catenoid end (see Figure 3 below) and is conformal to the first quadrant of the Schwartz-Christoffel Maps, which map the upper half plane conformally onto a polygonal shaped domain, for instance a square. In higher dihedral symmetry[9], the Costa Minimal Surface

---

[5] Michele Emmer, "Minimal Surfaces and Architecture: New Forms," Springer (Nexus Netw J, 2012), https://link.springer.com/content/pdf/10.1007%2Fs00004-013-0147-7.pdf.

[6] nicolas, Joseph O'Rourke, and Otis Chodosh, "Intuition for Mean Curvature," MathOverflow (Math Overflow, December 28, 2012), https://mathoverflow.net/questions/117460/intuition-for-mean-curvature.

[7] Mark Weaver, "Tension Fabric: Waves of the Future," USC Viterbi School of Engineering, July 21, 2005, https://illumin.usc.edu/tension-fabric-waves-of-the-future/.

[8] "The Costa Minimal Surface," The Costa Surface, accessed May 26, 2022, https://minimal.sitehost.iu.edu/essays/costa/index.html.

[9] Simply speaking, a regular polygon with n sides contains 2n different symmetries (n reflections and n rotations). A combination of reflections and rotations of a polygon make up a dihedral group of the polygon. Here, dihedral symmetries of the Costa Minimal Surface include its rotations and reflections with respect to different axes and planes, which in turn generalize to the Costa-Hoffman-Meeks Surface.

generalizes to the Costa-Hoffman-Meeks Surface. A Costa-Hoffman-Meeks Surface with dihedral symmetry n has genus n-1.[10]

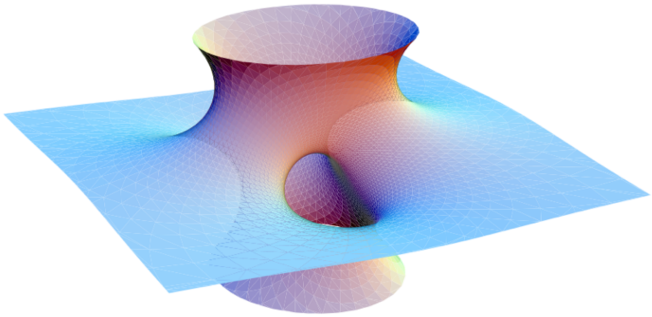

Figure 2. A Costa Minimal Surface with genus 1

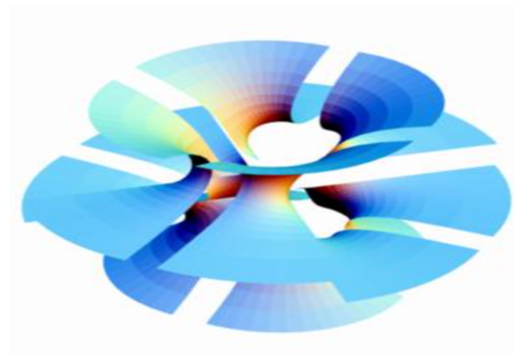

Figure 3. Eight Congruent Pieces of the Costa Surface

Francesco Polvi, an architect and researcher, expert in computational design and additive manufacturing at Institute for Advanced Architecture of Catalonia, designed the concept of an observatory utilizing Costa Minimal Surfaces from 2019 to 2020.[11] Since the Costa Minimal Surface is a minimal surface with mean curvature $H = 0$ everywhere, it brings the many advantages of minimal surfaces, such as conserving construction material and making the building frame lighter. From Figure 4 below, we can see that the final geometry of the building consists of an array of Costa Minimal Surfaces with various heights and rotations. It has genus 3 and is anchored in one plane, while the striping is two-directional. The geometry of the Costa Minimal Surfaces allows the interior and exterior parts of the observatory to be interconnected. As the interior and the exterior of the observatory are interconnected, light can be collected and passed through from the outside to the inside of the observatory in great volume efficiently. Since the Costa Surface minimizes surface area within the bounded by the outer building frame, it maximizes the interior volume given the boundary of the building frame and creates a large space within the observatory, which in turn enables light to be reflect off of multiple surfaces within the observatory and enhances the brightness within the structure. As Polvi plans to place the observatory beside a lake with sufficient lighting, the observatory should harbor a lot of sunlight in its large interior space, while its construction process becomes a lot more convenient thanks to the minimal surface properties of the Costa Surfaces.

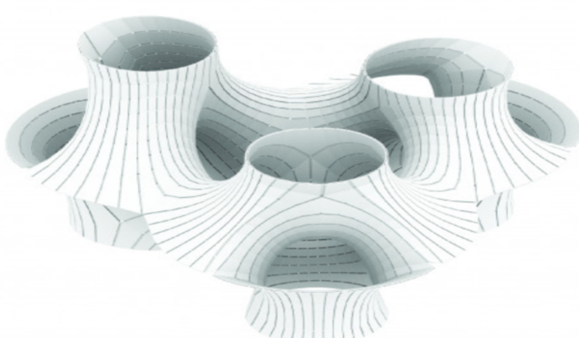

Figure 4. Design Concept of the Polvi Observatory

Figure 5. Concept Art of the Polvi Observatory

The Helicoid and the Spiral Staircase

A helicoid is a ruled surface swept out by a straight line that rotates at constant speed about an axis perpendicular to the line while simultaneously moving at constant speed along the axis. Consider the helicoid given

[10] "Costa-Hoffman-Meeks Surface," Costa-Hoffman-Meeks surface, 2004, https://virtualmathmuseum.org/Surface/costa-h-m/costa-h-m.html.
[11] Francesco Polvi, "Minimal Surface / Complex Forming," IAAC Blog, March 20, 2020, https://www.iaacblog.com/programs/minimal-surface-complex-forming/.

by the parametrization $\sigma(u, v) = (v \cos u, v \sin u, \lambda u)$. We calculate the coefficients of the first fundamental form to be $E = \lambda^2 + v^2, F = 0, G = 1$, and the coefficients of the second fundamental form to be $L = 0, M = \frac{\lambda}{\sqrt{\lambda^2+v^2}}, N = 0$. Then, the Weingarten Map is given by $W = \begin{bmatrix} 0 & \frac{\lambda}{\sqrt{\lambda^2+v^2}} \\ \frac{\lambda}{(\lambda^2+v^2)^{3/2}} & 0 \end{bmatrix}$. Then, the principal curvatures, the eigenvalues of W, are given by $\kappa_1 = \frac{\lambda}{\lambda^2+v^2}$ and $\kappa_2 = -\frac{\lambda}{\lambda^2+v^2}$. We verify that the mean curvature is given by $H = \frac{1}{2}(\kappa_1 + \kappa_2) = 0$ everywhere on the helicoid, meaning that the helicoid is a minimal surface. From Figure 6 below, we can see the lines of curvature (which align with the direction of principal vectors), which cross paths orthogonally everywhere on the helicoid.[12] Therefore, the figure allows us to geometrically grasp the idea of how the mean curvature is zero everywhere. As lines of curvature intersect orthogonally and the mean curvature equals 0, we can also imagine how surface tension is at equilibrium at every point on the helicoid (forces cancel in different directions) and how the helicoid is energy-conserving.

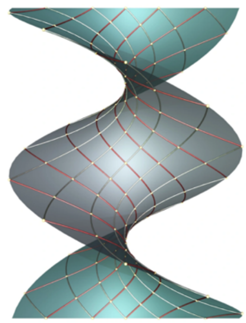

Figure 6. Lines of Curvature (Orthogonally Crossed) on a Helicoid. Note that the principal vectors point in the direction of the lines of curvature at every point on the helicoid.

In architecture, helicoids have been very frequently used in staircases, such as in the glass staircase shown in Figure 7 below. Generally speaking, spiral staircases turn around a central pole. Similar to the staircase below, helicoid staircases typically have a handrail on the outside.[13] Since the helicoid is a minimal surface, a helicoid staircase with a central pole is very space efficient in the use of floor area, thus making use of minimal construction material. However, a helicoid staircase does need to take caution in steep ascension or descension. Even when the helicoid staircase has a very large central column, the circumference of the circle at the walk line on the helicoid staircase needs to be small enough to avoid a normal tread depth and a normal rise height without compromising headroom (in our parametrization, this is controlled through adjusting λ and v). Many helicoid staircases have high rises to ensure sufficient headroom and a rather short going.

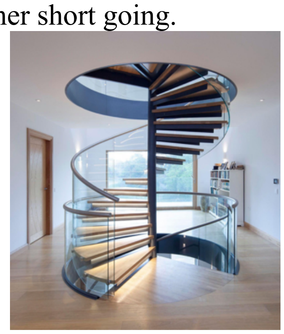

Figure 7. A Typical Helicoid Staircase

---

[12] "Principal Curvatures," The Inner Frame (Wordpress, August 6, 2016), https://theinnerframe.org/tag/principal-curvatures/.

[13] Inzerillo, Laura. 2012. "Helicoid and Architectural Application". DISEGNARECON 5 (10):219-24. https://doi.org/10.6092/issn.1828-5961/3348.

The staircase above is a closed right ruled generalized helicoid, which means that the profile curve intersects its axis of rotation orthogonally. Down the middle of the helicoid staircase is a geodesic, as shown in Figure 8 below. This has tremendous use in ancient times. In the medieval times, helicoid staircases often spiral clockwise from an ascender's point of view, making the attacking swordsmen, often right-handed, at a disadvantage, while the defenders could rush down the staircase through the geodesic (the central geodesic represents a shortest path between the upper and lower level of the helicoid staircase) to engage attackers with increased mobility (see Figure 9 below).[14]

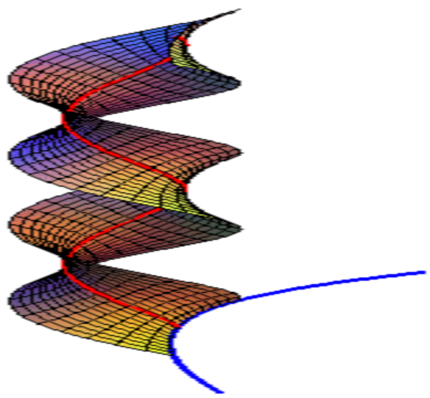

Figure 8. A Geodesic Down the Center of a Helicoid.

Figure 9. Ancient Helicoid Staircase in a Stone Castle

Of course, the closed right ruled generalized helicoid is not the only kind of helicoid staircase, as the helicoid is developable (a developable surface is a surface that can be flattened onto a plane without distortion). The entrance of the Louvre by the Pyramid is a famous example of a staircase of the shape of a developable helicoid (see Figure 10 below).[15] A developable helicoid is a surface of equal slope and is generated by a line of a rolling plane without sliding on a cylinder of revolution. The level curves of the developable helicoid are involute of circles and its lines of curvature are generatrices and its level curves. Compared to a closed right ruled generalized helicoid, a developable helicoid can offer a wider range of space on its walkline, create a more comfortable headspace, and provide a longer going without compromising headspace. Aesthetically, developable helicoids may suit the needs of more luxurious settings, though they are much harder to construct and measure.

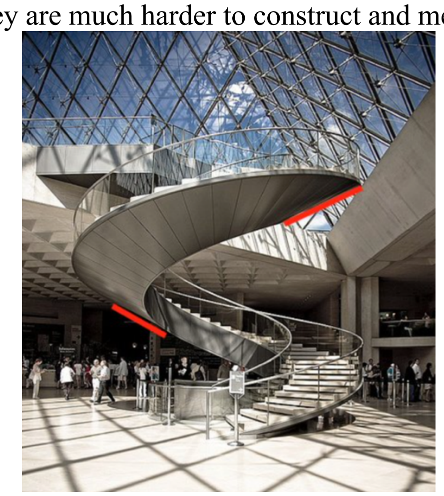

Figure 10. Developable Helicoid Staircase in the Louvre (the red lines mark generatrices, which are lines of curvature)

[14] Robert Ferreol, "Minimal Helicoid," Mathcurve, 2017, https://mathcurve.com/surfaces.gb/helicoidminimal/helicoidminimal.shtml.
[15] Robert Ferreol, "Developable Helicoid," Mathcurve, 2017, https://mathcurve.com/surfaces.gb/helicoiddeveloppable/helicoiddeveloppable.shtml.

Conclusion

As Tobias Wallisser exclaimed, “Mathematics can play a role in both parts, as overall conceptual inspiration for the generation of ideas and as tool for the geometrical relationships of elements.” As we have seen from both ancient and modern building structures utilizing minimal surfaces such as the Costa Minimal Surface and different helicoids, minimal surfaces have gradually increased their appearances and role in the world of architecture. Nowadays, more and more architects advocate for natural elements in their design, and minimal surfaces, a reoccurring theme in the natural world, certainly fit the needs of modern architects well. With the enhancement of computer science, simulation, and engineering technology, more and more geometric ideas are able to be realized and infused in architecture. Indeed, minimal surfaces have not only bridged mathematics and architecture, but moreover bonded the human race to nature.

Bibliography

"The Costa Minimal Surface." The Costa Surface. Accessed May 26, 2022. https://minimal.sitehost.iu.edu/essays/costa/index.html.

"Costa-Hoffman-Meeks Surface." Costa-Hoffman-Meeks surface, 2004. https://virtualmathmuseum.org/Surface/costa-h-m/costa-h-m.html.

Emmer, Michele. "Minimal Surfaces and Architecture: New Forms." Springer. Nexus Netw J, 2012. https://link.springer.com/content/pdf/10.1007%2Fs00004-013-0147-7.pdf.

Ferreol, Robert. "Developable Helicoid." Mathcurve, 2017. https://mathcurve.com/surfaces.gb/helicoiddeveloppable/helicoiddeveloppable.shtml.

Ferreol, Robert. "Minimal Helicoid." Mathcurve, 2017. https://mathcurve.com/surfaces.gb/helicoidminimal/helicoidminimal.shtml.

Hosch, William L. "Plateau Problem." Encyclopædia Britannica. Encyclopædia Britannica, inc. Accessed May 26, 2022. https://www.britannica.com/science/Plateau-problem.

Inzerillo, Laura. 2012. "Helicoid and Architectural Application". DISEGNARECON 5 (10):219-24. https://doi.org/10.6092/issn.1828-5961/3348.

Klarreich, Erica. "Math Duo Maps the Infinite Terrain of Minimal Surfaces." Quanta, March 12, 2019. https://www.quantamagazine.org/math-duo-maps-the-infinite-terrain-of-minimal-surfaces-20190312/.

Meadows, Alex. "Minimal Surfaces and Isoperimetric Problems in Mathematics." Soap film geometry, 2006. http://faculty.smcm.edu/ammeadows/create/.

nicolas, Joseph O'Rourke, and Otis Chodosh. "Intuition for Mean Curvature." MathOverflow. Math Overflow, December 28, 2012. https://mathoverflow.net/questions/117460/intuition-for-mean-curvature.

Photoeverywhere. "Photo: Flight of Spiral Stone Stairs." Photoeverywhere. Accessed May 26, 2022. https://photoeverywhere.co.uk/britain/york/slides/09-yorkspiral3.htm.

Polvi, Francesco. "Minimal Surface / Complex Forming." IAAC Blog, March 20, 2020. https://www.iaacblog.com/programs/minimal-surface-complex-forming/.

Pressley, Andrew. *Elementary Differential Geometry*. 2nd ed. Springer, 2012.

"Principal Curvatures." The Inner Frame. Wordpress, August 6, 2016. https://theinnerframe.org/tag/principal-curvatures/.

Schwarz-Christoffel Maps. Accessed May 26, 2022. https://minimal.sitehost.iu.edu/essays/christoffel/index.html.

"Spiral Staircase." Accessed May 26, 2022. https://www.made-in-china.com/products-search/hot-china-products/Stainless_Steel_Spiral_Staircase.html.

Weaver, Mark. “Tension Fabric: Waves of the Future.” USC Viterbi School of Engineering, July 21, 2005. https://illumin.usc.edu/tension-fabric-waves-of-the-future/.